Biotherapy of B-Cell Precursor Leukemia by Targeting Genistein to CD19-Associated Tyrosine Kinases

F. M. Uckun,* W. E. Evans, C. J. Forsyth, K. G. Waddick, L. T.-Ahlgren, L. M. Chelstrom, A. Burkhardt, J. Bolen, D. E. Myers

B-cell precursor (BCP) leukemia is the most common form of childhood cancer and the second most common form of acute leukemia in adults. Human BCP leukemia was treated in a severe combined immunodeficient mouse model by targeting of the tyrosine kinase inhibitor Genistein (Gen) to the B cell–specific receptor CD19 with the monoclonal antibody B43. The B43-Gen immunoconjugate bound with high affinity to BCP leukemia cells, selectively inhibited CD19-associated tyrosine kinases, and triggered rapid apoptotic cell death. At less than one-tenth the maximum tolerated dose more than 99.999 percent of human BCP leukemia cells were killed, which led to 100 percent long-term event-free survival from an otherwise invariably fatal leukemia. The B43-Gen immunoconjugate might be useful in eliminating leukemia cells in patients who have failed conventional therapy.

Src protooncogene family protein tyrosine kinases (PTKs) play a pivotal role in vital functions of human cells (*1*). Attempts have been made to develop anticancer agents that are specific inhibitors of Src-family PTKs (*2*). Although some Lck-specific inhibitors were developed with potent inhibitory activity to isolated Lck, they could not be delivered to cancer cells efficiently enough to cause cytotoxicity (*2*). Cancer cells express several members of the Src PTK family that share most of their substrates (*1*). Therefore, compensation by other members of the Src PTK family in cancer cells would render such highly specific inhibitors ineffective as anticancer agents. Similarly, antisense depletion of a particular Src-family PTK is unlikely to prove effective as a cancer treatment modality because of the aforementioned complementation by other active members of the Src PTK family (*3*). Here we report an alternative strategy that allows the targeting of a general PTK inhibitor (one that inhibits all members of the Src PTK family) to cancer cells. The targeting of the kinase inhibitor is achieved with an antibody that recognizes a receptor on the surface of cancer cells that is physically associated with the Src-family PTKs. We demonstrate the feasibility of this approach using BCP leukemia, the most common form of childhood cancer (*4*), as a model system.

The CD19 molecule is a B lineage–specific surface receptor that is expressed on the surface of leukemia cells from 85% of patients with acute lymphoblastic leukemia (ALL). It is absent from the parenchymal cells of nonhematopoietic organs, circulating blood myeloid and erythroid cells, T cells, and bone marrow stem cells (*5*, *6*), thereby reducing the opportunity for nonspecific toxicity when antibodies to CD19 are used in biotherapy. $CD19^+$ ALLs are believed to originate from putative developmental lesions in normal B cell precursor (BCP) clones during early phases of ontogeny and are therefore classified as BCP leukemias (*4*, *7*). CD19 is found on the surface of each BCP leukemia cell at a high density (>50,000 molecules per cell) and shows a high affinity for the monoclonal antibody (mAb) B43 (anti-CD19) ($K_a > 10^8\ M^{-1}$) (*5*). The receptor is not shed from the cell surface and undergoes antibody-induced internalization upon binding of B43 (*5*). CD19 is physically and functionally associated with Src protooncogene family PTKs Lyn, Lck, Fyn, and Blk to form transmembrane receptor tyrosine kinases with ancillary signal-transducing functions (*8*). Src-family PTKs in these CD19 receptor–PTK complexes act as signal transducers and couple CD19 to downstream cytoplasmic signaling pathways (*8*, *9*). Because Src-family PTKs are abundantly expressed in B-lineage leukemia cells (*1*), we postulate that the CD19 receptor may be a suitable target for biotherapy with PTK inhibitors.

Genistein (Gen), an isoflavone (5,7,4′-trihydroxyisoflavone) derived from fermentation broth of *Pseudomonas* spp., is a naturally occurring tyrosine kinase inhibitor present in soybeans (*10*). Gen inhibits purified Lck kinase from human lymphoid cells at micromolar concentrations (*11*). We conjugated Gen to mAb B43 by photoaffinity cross-linking using the photosensitive 18.2 Å long noncleavable heterobifunctional cross-linking agent sulfosuccinimidyl 6-[4′-azido-2′-nitrophenylamino] hexanoate (Sulfo-SANPAH) to generate a CD19-directed, B lineage–specific PTK inhibitor (*12*, *13*) (Fig. 1A). The selective immunoreactivity of B43-Gen with BCP leukemia cells was confirmed by standard ligand-binding assays (*14*). $CD19^+$ BCP leukemia cells specifically bound $2.7 \pm 0.2 \times 10^4$ molecules of the immunoconjugate at in vivo–achievable saturating concentrations, whereas no detectable binding to $CD19^-$ myelogenous or T-lineage leukemia cells was observed (*14*). We examined the binding of B43-Gen to $CD19^+$ BCP leukemia cells by flow cytometry with fluorescein isothiocyanate (FITC)–labeled goat antibodies to the mouse immunoglobulin moiety of the immunoconjugate. B43-Gen stained BCP leukemia cells with the same intensity as unconjugated B43 over a broad range of concentrations; it competed as effectively as unconjugated B43 with phycoerythrin (PE)–labeled B43 or mAb Leu12 (anti-CD19) for surface binding sites (*15*).

Most Src-family PTK activity in B-lineage leukemia cells is membrane-associated as a result of the myristylation of the PTK NH_2-terminus, whereas the remainder is largely cytoplasmic (*1*). Therefore, a Gen-containing immunoconjugate that localizes to the membrane as well as cytoplasm would be more likely to reduce the total CD19-associated Src PTK activity than an immunoconjugate that is rapidly internalized and does not remain bound to the membrane. The destination of surface-bound B43–^{125}I-Gen was traced in $CD19^+$ BCP leukemia cell lines NALM-6 and NALM-16 (*16*, *17*). Leukemia cells were homogenized after 18 hours of treatment with the immunoconjugate, and various subcellular components were fractionated on Percoll density gradients.

A substantial portion of B43–^{125}I-Gen, representing 39% of the total cpm recovered from the in situ–generated Percoll gradient, was localized in the plasma membrane or Golgi compartments of NALM-6 cells, as confirmed by cosedimentation with 5′-nucleotidase (a marker for the plasma membrane) and galactosyltransferase (a marker for the Golgi) (Fig. 1B). The remainder of radioactivity representing internalized B43–^{125}I-Gen was associated with the soluble cytoplasmic fraction (15% of total cpm; Percoll

F. M. Uckun, Biotherapy Program, Departments of Therapeutic Radiology–Radiation Oncology, Pediatrics, and Pharmacology, and the Centralized Immunoconjugate Reference Laboratory of the Childrens Cancer Group, University of Minnesota, Minneapolis, MN 55455, USA.
W. E. Evans, Pharmaceutical Department, St. Jude Children's Research Hospital, Memphis, TN 38101, USA.
C. J. Forsyth, Department of Chemistry, University of Minnesota, Minneapolis, MN 55455, USA.
K. G. Waddick, L. T. Ahlgren, L. M. Chelstrom, D. E. Myers, Biotherapy Program, Department of Therapeutic Radiology–Radiation Oncology, University of Minnesota, Minneapolis, MN 55455, USA.
A. Burkhardt and J. Bolen, Signal Transduction Laboratory, Department of Molecular Biology, Bristol-Myers Squibb Pharmaceutical Research Institute, Princeton, NJ 08543, USA.
* To whom correspondence should be addressed.

gradient fractions 1 to 3; density <1.043 g/ml), endoplasmic reticulum (26% of total cpm; Percoll gradient fractions 10 to 19; density range, 1.049 to 1.056 g/ml), and lysosomes (14% of total cpm; Percoll gradient fractions 20 to 25; density range, 1.056 to 1.069 g/ml). Similar results were obtained with NALM-16 cells (Fig. 1B).

We next assessed the inhibitory effects of B43-Gen on Src-family PTKs. Lyn and Lck, the predominant members of the Src PTK family in BCP leukemia cells (*1*, 8), were immunoprecipitated from Nonidet P-40 lysates of RAMOS and NALM-6 cells, and their enzymatic activity, as measured by autophosphorylation, was evaluated after a 4-hour incubation in the presence of B43-Gen. B43-Gen, but not unconjugated B43, inhibited Lyn and Lck kinases at nanomolar concentrations (Fig. 2, A and B). By comparison, topoisomerase II enzyme was not inhibited even at micromolar concentrations of B43-Gen (*18*).

CD19 is physically and functionally associated with Lyn and Lck kinases (8). To examine whether B43-Gen might inhibit the CD19-associated Src-family PTKs after binding to CD19, we treated NALM-6 cells, which express high concentrations of Lyn, and RAMOS cells, which express high concentrations of Lck (8), with nanomolar concentrations of the immunoconjugate for 4 hours and estimated the PTK activities of Lyn and Lck by immune complex protein kinase assays (*19*). Control cells were treated with unconjugated Gen, mAb TXU-Gen immunoconjugate directed to the CD7(Tp41) T cell surface molecule, unconjugated and unmodified mAb B43, or SANPAH-modified, unconjugated mAb B43.

B43-Gen treatment at nanomolar concentrations resulted in inhibition of Lyn and Lck kinases, as reflected by decreased autophosphorylation or enolase substrate phosphorylation (Fig. 2, C and D). The abundance of the enzyme, as determined by anti-Lyn immunoblotting, did not change during the course of the experiment, which is consistent with decreased specific activity. Inhibition of Lyn kinase after B43-Gen treatment was associated with decreased tyrosine phosphorylation of abundant protein substrates in NALM-6 cells, as determined by immunoblotting with a polyclonal antibody to phosphotyrosine (*20*). In contrast, micromolar concentrations of unconjugated Gen did not affect the enzymatic activity of Lyn or the baseline phosphorylation status of tyrosine-phosphorylated proteins. Thus, the B43-Gen immunoconjugate was over 1500 times more effective than unconjugated Gen at inhibiting Lyn kinase and causing decreased tyrosine phosphorylation in NALM-6 cells (*20*). Unlike B43-Gen, neither unconjugated mAb B43 (derivatized or underivatized) nor the control immunoconjugate TXU-Gen inhibited Lyn or Lck kinases (Fig. 2, C and D), indicating that both the tyrosine kinase–inhibitory Gen moiety and the CD19-specific B43 mAb moiety are required for the B43-Gen–induced inhibition of Src-family PTKs in BCP leukemia cells.

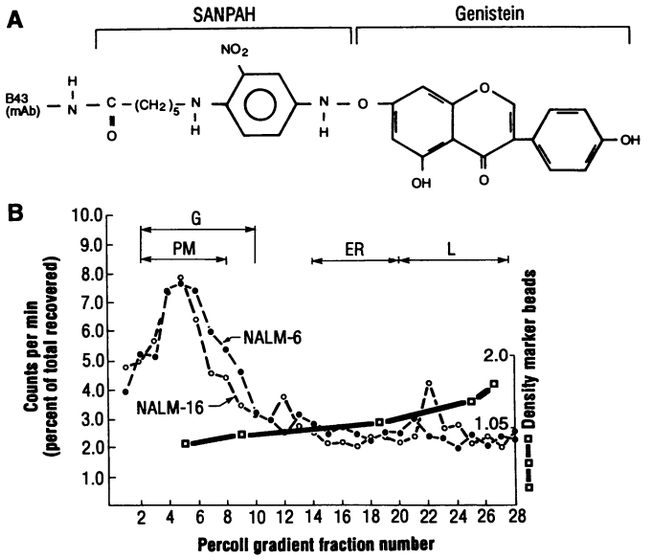

Fig. 1. (**A**) Structure of the B43-Gen immunoconjugate. One molecule of Gen was conjugated to one molecule of mAb B43 through use of the SANPAH cross-linker (*12*, *13*). (**B**) Fate of cell-bound B43-Gen immunoconjugate. Pellets of CD19$^+$ NALM-6 and NALM-16 BCP leukemia cells were incubated with B43–^{125}I-Gen (1.8 × 10^5 cpm/nmol) for 18 hours at 37°C (660 pmol/10^8 cells), washed to remove unbound immunoconjugate, and homogenized, and various subcellular components were fractionated on density gradients of colloidal silica (Percoll) (*16*). Density marker beads were used to determine gradient density. The indicated gradient regions for plasma membranes (PM), Golgi (G), endoplasmic reticulum (ER), and lysosomes (L) were determined on the basis of the characteristic distribution profile of the marker enzymes 5′-nucleotidase, galactosyltransferase, neutral α-glucosidase, and hexosamidase, respectively (*17*).

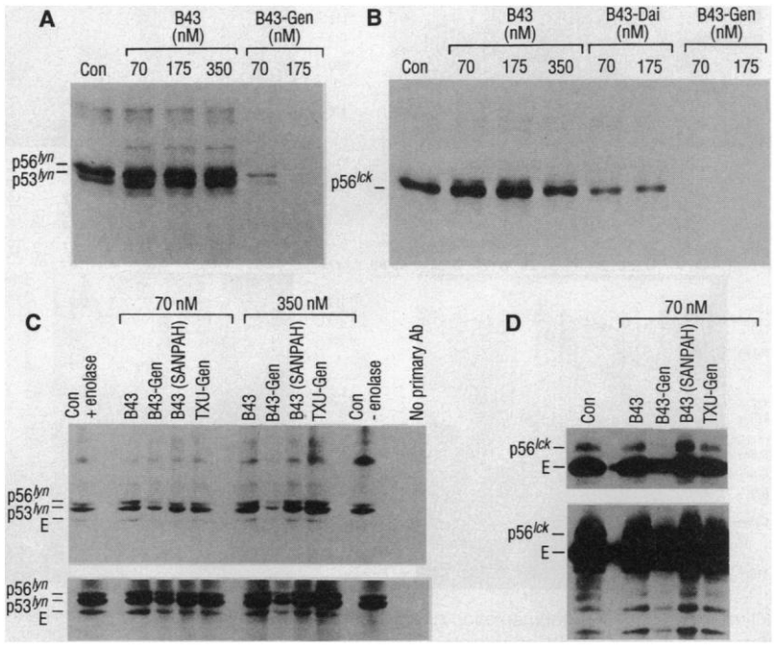

Fig. 2. Inhibitory activity of B43-Gen immunoconjugate on Src-family PTKs of CD19$^+$ leukemia cells. (**A** and **B**) The kinase activities of Lyn immunoprecipitated from NALM-6 pre-B acute lymphoblastic leukemia cells and Lck immunoprecipitated from RAMOS Burkitt's leukemia–lymphoma cells were determined before and after a 4-hour incubation with B43-Gen or Sulfo-SANPAH–modified mAb B43 during a 10-min kinase reaction in the presence of [γ-^{32}P]ATP (50 μCi/μmol) (*8*). (**C** and **D**) NALM-6 and RAMOS cells were treated for 4 hours at 37°C with the indicated concentrations of B43-Gen, pelleted, and lysed in NP-40 lysis buffer, and immune complex kinase assays of Lyn activity in NALM-6 cells and Lck activity in RAMOS cells were performed with acid-denatured rabbit enolase as an exogenous PTK substrate (*8*). Control reagents included unmodified mAb B43, Sulfo-SANPAH–modified mAb B43, and TXU-Gen immunoconjugate, which does not react with CD19$^+$ leukemia cells.

B43-Gen inhibited Lyn kinase in K562 erythroleukemia cells transfected with human CD19 complementary DNA (cDNA), but it did not inhibit Lyn kinase in untransfected K562 erythroleukemia cells or stable K562 transfectants expressing the CD19 deletion mutant A308, which is truncated on exon 6 and has no tyrosine residues that allow association with the Src homology domain 2 of Lyn (*21*). Thus, B43-Gen inhibited Lyn kinase only if this kinase was associated with the CD19 receptor. Syk kinase, which is not directly associated with the CD19 receptor in unstimulated leukemia cells, was not inhibited after treatment of NALM-6 cells with B43-Gen (*22*). Similarly, PKC and PKC-dependent renaturable serine kinases were not inhibited by B43-Gen even at a concentration of 350 nM (*22*). Thus, the B43-Gen immunoconjugate was a potent and cell type–specific PTK inhibitor that selectively inhibited CD19-associated PTK in $CD19^+$ leukemia cells.

Apoptosis, also known as programmed cell death, is a common mode of eukaryotic cell death characterized by distinct ultrastructural features and a ladder-like DNA fragmentation pattern produced by endonuclease-mediated cleavage of DNA into oligonucleosome-length fragments (*23*). Ionizing radiation and chemotherapeutic drugs with diverse molecular targets, such as prednisone, cisplatin, methotrexate, L-asparaginase, etoposide, 5-fluorouracil, and cyclophosphamide induce apoptotic cell death in human cells (*19*, *23*). Protein tyrosine kinases participate in initiation of signal cascades that regulate Bcl-2 oncoprotein expression and apoptosis in human hematopoietic cells (*19*, *23*). Therefore, we investigated whether inhibition of Src-family PTKs induced by B43-Gen could trigger apoptosis in B-lineage leukemia cells. B43-Gen caused apoptosis of NALM-6 cells within 8 hours; distinctive morphologic changes were seen by light microscopy. Indications of extensive cellular damage included shrinkage, nuclear chromatin condensation, segmentation of the nucleus, and plasma membrane blebs in >75% of cells.

On agarose gels, DNA from B-lineage leukemia cells treated with nanomolar concentrations of B43-Gen for 8 to 24 hours showed a ladder-like fragmentation pattern consistent with an endonucleolytic cleavage of DNA into oligonucleosome-length fragments at multiples of 200 base pairs, whereas DNA from cells treated with micromolar concentrations of unconjugated Gen showed no fragmentation (Fig. 3, A and B). The B43-Gen immunoconjugate induced apoptosis in highly radiation-resistant RS4;11 leukemia cells, which express high amounts of Bcl-2 oncoprotein (Fig. 3A). Apoptosis of leukemia cells was triggered by the Gen moiety of the immunoconjugate, because high concentrations of unconjugated Gen but not unconjugated mAb B43 induced DNA fragmentation (Fig. 3B). The B43-Gen–induced apoptosis was CD19-specific because (i) control immunoconjugate TXU-Gen did not induce

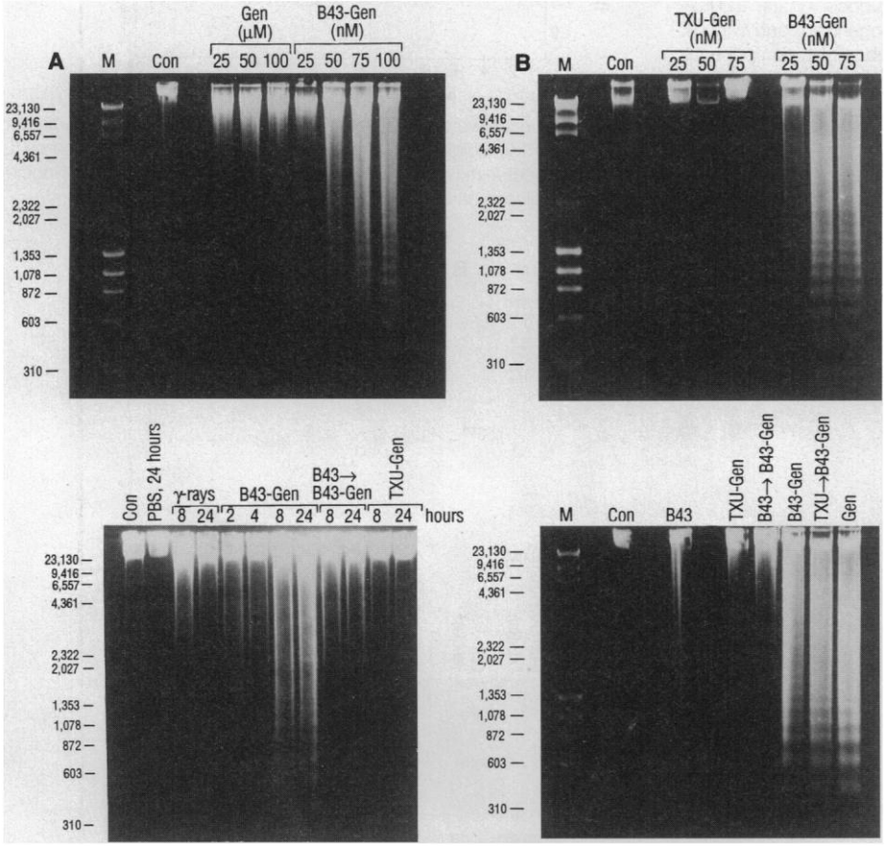

Fig. 3. Internucleosomal DNA fragmentation in B43-Gen–treated leukemia cells. Cells were harvested 24 hours after exposure to the B43-Gen immunoconjugate, and DNA was prepared for analysis of fragmentation. DNA was then separated by electrophoresis through a 1% agarose gel, and the DNA bands were visualized by UV light after staining with ethidium bromide. (**A**) (**Upper panel**) RS4;11 cells (*25*) were treated with unconjugated Gen or B43-Gen immunoconjugate for 24 hours at 37°C. (**Lower panel**) RS4;11 cells were treated with PBS, 2 Gy of γ-rays, 75 nM B43-Gen with and without prior incubation in the presence of 10-fold molar excess of unconjugated mAb B43, or 75 nM TXU-Gen. (**B**) (**Upper panel**) NALM-6 cells were treated with B43-Gen or TXU-Gen for 24 hours. (**Lower panel**) NALM-6 cells were treated for 24 hours with 75 nM B43-Gen, 75 nM TXU-Gen, 100 μM unconjugated Gen, or 750 nM unconjugated B43. In addition, controls included DNA from cells treated with 750 nM unconjugated B43 or TXU for 1 hour on ice before treatment with the immunoconjugate. Lane M, molecular size markers (in base pairs).

Table 1. Tissue distribution parameters for tyrosine kinase inhibitors in SCID mice. A flow-limited physiological pharmacokinetic model was used to characterize the tissue disposition of both drugs in mice. Volume terms and flow rates were those previously described for mice (*28*). A set of differential equations describing the mass balances of each model compartment was used to estimate linear binding constants for each organ and clearance rates. These differential equations were simultaneously solved with the use of ADAPT II software (*27*). *R*, tissue-to-plasma equilibrium distribution ratio for linear binding.

Tissue	B43-Gen		Gen
	No leukemia	End-stage leukemia	No leukemia
Linear binding constant (R)			
Lungs	0.221	0.339	0.531
Brain	0.008	0.012	0.027
Heart	0.117	0.236	0.335
Skin	0.061	0.10	0.208
Spleen	0.145	0.323	0.040
Kidney	0.118	0.162	0.253
Muscle	0.016	0.028	0.085
Femur	0.031	0.109	0.00008
Liver	0.139	0.290	0.50
Rest of body*	0.033	0.055	1.11
Clearance (μl hour^{-1} g^{-1})			
Kidney	0.56	1.4	18.7
Liver	1.2	1.2	40.9
Total clearance	1.76	2.6	59.6

*Residual amount of drug not accounted for by tissues studied.

apoptosis (Fig. 3, A and B) and (ii) cell death was prevented by prior incubation of CD19$^+$ leukemia cells with a 10-fold molar excess of unconjugated mAb B43 but not with a 10-fold molar excess of mAb TXU

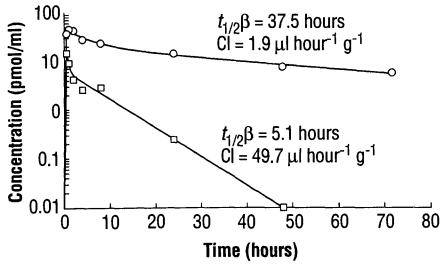

Fig. 4. Pharmacokinetic features of B43 (anti-CD19)–Gen immunoconjugate. After intravenous injection of B43–^{125}I-Gen (1.8 × 10^5 cpm/nmol) or ^{125}I-Gen (2.6 × 10^5 cpm/nmol), SCID mice were serially bled by retroorbital venipuncture. A two-compartment first-order pharmacokinetic model was fit to the data for plasma concentration versus time (27). Plasma concentration versus time for B43-Gen immunoconjugate (○) and unconjugated Gen (□), after injection of 58 pmol into SCID mice. Lines represent two-compartment model simulations, symbols depict measured concentrations. $t_{1/2}\beta$, elimination half-life; Cl, systemic clearance from plasma.

(Fig. 3, A and B). Thus, the B43-Gen immunoconjugate is an active antileukemia agent in vitro.

We next examined the pharmacokinetic features of B43-Gen in a severe combined immunodeficient (SCID) mouse model of human BCP leukemia (26). The B43-Gen immunoconjugate has a substantially longer elimination half-life and slower plasma clearance than unconjugated Gen (Fig. 4). The immunoconjugate was cleared more rapidly from plasma (3.3 versus 1.9 μl hour^{-1} g^{-1}), had a shorter elimination half-life (20.5 versus 37.5 hours), and had a larger volume of distribution (63.9 versus 52.0 μl/g) in SCID mice with end-stage human BCP leukemia (that is, SCID mice with disseminated human BCP leukemia that, because of central nervous system involvement, were paralyzed) than in healthy SCID mice that were not inoculated with leukemia cells. Thus, the B43-Gen immunoconjugate binds to CD19$^+$ leukemia cells infiltrating SCID mouse tissues, resulting in more rapid removal of the immunoconjugate from plasma in mice with end-stage leukemia.

This hypothesis was supported by measurement of higher concentrations of the immunoconjugate in tissues of SCID mice with end-stage leukemia, when compared to healthy SCID mice that were not inoculated with leukemia cells (Table 1). Spleen, liver, and lungs had the highest tissue-to-plasma ratio, with the tissue distribution ratio increasing approximately two times in the spleen and liver of mice with end-stage leukemia (Table 1). Although tissue distribution of the immunoconjugate into femur was low in mice with a minimal leukemia burden, it increased three times in mice with end-stage leukemia, most likely reflecting binding of the immunoconjugate to CD19-positive human B-lineage leukemia cells infiltrating the bone marrow. Lower tissue concentrations of unconjugated Gen indicate that it is cleared from the body more rapidly than the B43-Gen immunoconjugate. The total systemic clearances of Gen and B43-Gen estimated by the physiological model (Table 1) were in close agreement with clearances estimated by the two-compartment operational model (Fig. 4).

B43-Gen was not toxic to SCID mice at doses ranging from 10 μg (67 pmol) to 250 μg (1667 pmol). None of the 42 mice treated with B43-Gen experienced side effects or

Table 2. Antileukemic activity of B43–Gen immunoconjugate against human BCP leukemia in SCID mice. SCID mice were inoculated intravenously with 1 × 10^6 NALM-6 leukemia cells. After 24 hours, mice received antileukemic therapy according to the indicated protocols. Controls were treated with unconjugated Gen (10 μg per mouse), unconjugated B43 (50 μg per mouse), or PBS qd × 3 d. All drugs and PBS were administered parenterally. Chemotherapeutic drugs were used at clinically applied high doses. B43, mAb to CD19; TXU, mAb to CD7; J3-109, mAb to CD72; Gen, Genistein; Dai, daidzein (Gen analog); PAP, pokeweed antiviral protein; qd, every day; EFS, event-free survival; AUC_{0-3}, area under curve; qwk, every week; IU, international units; qod, every other day; TBI, total body irradiation; BMT, bone marrow transplant.

Treatment group	Schedule	Number of mice	EFS (%)		Median EFS (days)	*P* (versus B43-Gen)
			60 days	120 days		
Control	See legend	110	1	0	39	<0.00001
		PTK inhibitors				
B43–Gen	12.5/25 mg m^{-2} qd × 3 d	10	100	100	>120	–
TXU–Gen	25 mg m^{-2} qd × 3 d	10	0	0	44	<0.00001
B43–Dai	12.5/25 mg m^{-2} qd × 3 d	10	60	20	81	<0.00001
		Alkylating agents				
Cyclophosphamide	300 mg m^{-2} qd × 10 d	10	40	10	54	<0.00001
Carmustine	150 mg m^{-2} × 1	5	20	0	54	<0.00001
		Topoisomerase inhibitors				
Etoposide*	1.7 mg m^{-2} × 1	10	60	30	66	<0.00001
Topotecan†	150 mg m^{-2} 72 h^{-1}	10	18	0	44	<0.00001
		Antimetabolites				
Cytarabine	300 mg m^{-2} qd × 10 d	5	20	0	57	<0.00001
		Mitotic inhibitors				
Taxol	60 mg m^{-2} qd × 5 d	10	0	0	37	<0.00001
Vincristine	30 mg m^{-2} qwk × 4	5	0	0	51	<0.00001
		Immunotoxins				
B43–PAP	10 mg m^{-2} qd × 3 d	20	90	55	>120	<0.01
J3-109–PAP	15 mg m^{-2} qd × 3 d	10	20	0	51	<0.00001
		Other agents				
Methylprednisone	30 mg m^{-2} qd × 10 d	10	40	20	56	<0.00001
Doxorubicin	6 mg m^{-2} qd × 10 d	5	20	0	49	<0.00001
L-asparaginase	30,000 IU m^{-2} qod × 5	5	0	0	44	<0.00001
TBI	2.5 Gy→BMT	5	0	0	47	<0.00001

*Etoposide treatment at this maximum tolerated dose yields an AUC_{0-3} of 59.2 μM · hour ml^{-1}. †Topotecan treatment on this schedule yields a steady-state plasma concentration of 1.3 μg liter^{-1}.

died of toxicity during the 36-day observation period. No histopathologic lesions were found in the organs of B43-Gen–treated mice that were electively killed at ~37 days. Thus, the maximum tolerated dose (MTD) of B43-Gen was not reached at 250 μg per mouse (or 12.5 mg per kilogram of body mass). We next evaluated the antileukemic efficacy of B43-Gen against human B-lineage leukemia in SCID mice. All control mice treated with unconjugated Gen (10 μg per mouse; 37 nmol per mouse), unconjugated mAb B43 (50 μg per mouse), TXU-Gen control immunoconjugate (50 μg per mouse), or phosphate-buffered saline (PBS) died of disseminated human BCP leukemia at 24 to 61 days after inoculation (Table 2). In contrast, all mice treated with B43-Gen immunoconjugate at doses of 25 μg per mouse (<10% of the MTD) or 50 μg per mouse (<20% of the MTD) remained alive without clinical evidence of leukemia for >4 months.

The long-term–surviving mice were killed at 142 days to examine their burden of human leukemia cells. Postmortem histopathologic examination of tissue sections from multiple organs did not reveal any leukemic infiltrates. We found no molecular evidence of occult leukemia when DNA from bone marrow, spleen, liver, and brain meninges was examined for human β-globin gene sequences by polymerase chain reaction (PCR) (*29*). In contrast, diffuse leukemic infiltrates and PCR evidence of human DNA were found in bone marrow, liver, spleen, and meninges of SCID mice treated with PBS or TXU-Gen. A single NALM-6 cell will cause disseminated fatal leukemia in SCID mice (*26*). The absence of engrafted leukemia cells in B43-Gen–treated SCID mice 20 weeks after inoculation of 1×10^6 NALM-6 cells indicates that at nontoxic doses this immunoconjugate killed >99.999% of NALM-6 cells in vivo. Similar therapeutic efficacy could not be achieved by standard or investigational chemotherapeutic agents (Table 2), including the alkylating agents cyclophosphamide and carmustine, the topoisomerase II inhibitor etoposide, the topoisomerase I inhibitor topotecan, the antimetabolite cytarabine, mitotic inhibitors taxol and vincristine, pokeweed antiviral protein (PAP) immunotoxins to CD19 or CD72 pan–B cell antigens, methylprednisone, doxorubicin, L-asparaginase, or 250 cGy of total body irradiation. Another PTK inhibitory anti-CD19 immunoconjugate containing the Gen analog daidzein (Dai), which is a less potent PTK inhibitor than Gen (*10*), was not as effective as B43-Gen (Table 2).

The crystal structure of the Src-family PTK has not been determined. Therefore, little is known about any structure-activity relations with respect to isoflavones like Gen or any other PTK inhibitor. Gen does not easily enter cells and causes only a reversible inhibition of Src-family PTKs at micromolar concentrations. More Gen molecules were delivered into leukemia cells by the targeted biotherapy approach we described. Localization of the Gen molecule in close proximity to the adenosine triphosphate (ATP)–binding domains of Src-family PTKs may increase the effective binding constant by both reducing entropy and providing additional linker binding contacts and consequently lead to sustained inhibition of Src-family PTKs. This goal can be accomplished by conjugation of Gen to mAb B43, which binds to and remains complexed with CD19, which in turn is physically associated with the Src-family PTKs. Our results show that treatment of $CD19^+$ leukemia cells with nanomolar concentrations of B43-Gen immunoconjugate caused sustained inhibition of CD19-associated Src-family PTKs. Oxidation of Src-family PTKs reduces their enzymatic activity, which can be restored with reducing agents such as dithiothreitol (DTT) (*30*). The inhibitory activity of the B43-Gen immunoconjugate against Src-family PTKs in whole-cell lysates was also reduced in the presence of DTT (*31*). We therefore postulate that decreasing the effective off-rate of Gen by conjugating it to mAb B43 could enhance the likelihood of covalent modification of the CD19-associated Src-family PTKs. The conjugated neon moiety of Gen could act as a Michael acceptor.

Our data suggest that extranuclear signals are important in the induction of apoptosis. PTK inhibitors may have therapeutic potential in the treatment of hematologic malignancies. The B43-Gen immunoconjugate may offer an effective treatment for BCP leukemia. Its favorable pharmacodynamic features, superior cytotoxic activity against leukemia cells resistant to radiation as well as to several other established antileukemia agents, and lack of systemic toxicity recommend the clinical evaluation of this cell type–specific PTK inhibitor in BCP leukemia patients who have failed standard therapy. Preclinical (*32*) and clinical studies (*33*, *34*), especially the normal development of a functional $CD19^+$ B-lineage lymphoid compartment in recipients of autologous bone-marrow grafts depleted of $CD19^+$ BCP and mature B lymphocytes (*33*), and the lack of sustained B-cell immunosuppression in leukemia patients treated with an anti-CD19 immunotoxin (*34*), provide evidence that CD19 is not expressed on the surface of the most immature normal pro–B cell populations. Therefore, the B43-Gen immunoconjugate is not likely to cause sustained B-cell immunosuppression. During the B43-Gen–induced transient hypogammaglobulinemia, patients could be supported with intravenous immunoglobulin infusions. Whether immunoconjugates that contain Gen, such as B43-Gen, are superior to immunoconjugates containing cytotoxic drugs (*35*) or toxins (*34*, *36*) or to bispecific antibodies plus human T cells (*37*) should be examined in the appropriate clinical settings. In addition, laboratory studies should begin to examine whether targeted biotherapy using PTK-inhibitory immunoconjugates could also be applied to nonhematologic forms of human cancer. Finally, Gen-containing immunoconjugates could be useful as probing agents to identify surface receptors that are associated with vital PTK.

REFERENCES AND NOTES

1. J. B. Bolen *et al.*, *Adv. Can. Res.* **57**, 103 (1991); J. B. Bolen *et al.*, *FASEB J.* **6**, 3403 (1992).
2. T. Burke *et al.*, *J. Med. Chem.* **36**, 425 (1993); M. Cushman *et al.*, *ibid.* **37**, 3353 (1994); M. Cushman *et al.*, *ibid.* **34**, 798 (1991).
3. R. H. Scheuermann *et al.*, *Proc. Natl. Acad. Sci. U.S.A.* **91**, 4048 (1994).
4. M. F. Greaves, *Science* **234**, 697 (1986); M. F. Greaves, *Blood* **82**, 1043 (1993); F. M. Uckun *et al.*, *N. Engl. J. Med.* **329**, 1296 (1993); G. K. Rivera *et al.*, *ibid.*, p. 1289.
5. F. M. Uckun, K. J. Gajl-Peczalska, J. H. Kersey, L. L. Houston, D. A. Vallera, *J. Exp. Med.* **163**, 347 (1986); I. Stamenkovic and B. Seed, *ibid.* **168**,1205 (1988); F. M. Uckun *et al.*, *Blood* **71**, 13 (1988); T. F. Tedder and C. M. Isaacs, *J. Immunol.* **143**, 712 (1989).
6. F. M. Uckun and J. A. Ledbetter, *Proc. Natl. Acad. Sci. U.S.A.* **85**, 8603 (1988); J. A. Ledbetter, C. H. June, C. W. Song, E. A. Clark, F. M. Uckun, *ibid.*, p.1897; F. M. Uckun *et al.*, *ibid.* **88**, 3589 (1991).
7. L. M. Nadler *et al.*, *J. Immunol.* **131**, 244 (1983); F. M. Uckun, *Blood* **76**, 1908 (1990); F. M. Uckun *et al.*, *ibid.* **79**, 3369 (1992).
8. F. M. Uckun *et al.*, *J. Biol. Chem.* **268**, 21172 (1993).
9. A. K. Matsumoto *et al.*, *J. Exp. Med.* **173**, 55 (1991); R. H. Carter and D. T. Fearon, *Science* **256**, 105 (1992); D. A. Tuveson, R. H. Carter, S. P. Soltoff, D. T. Fearon, *ibid.* **260**, 986 (1993); R. E. Callard *et al.*, *J. Immunol.* **148**, 2983 (1992); L. E. Bradbury, V. S. Goldmacher, T. F. Tedder, *ibid.* **151**, 2915 (1993); N. J. Chalupny *et al.*, *EMBO J.* **12**, 2691 (1993).
10. H. Pettersson and K.-H. Kiessling, *J. Assoc. Off. Anal. Chem.* **67**, 503 (1984); T. Akiyama *et al.*, *J. Biol. Chem.* **262**, 5592 (1987); H. Adlercreutz *et al.*, *Clin. Chim. Acta.* **199**, 263 (1991); H. Adlercreutz *et al.*, *Am. J. Clin. Nutr.* **54**, 1093 (1991).
11. J. M. Trevilyan *et al.*, *J. Immunol.* **145**, 3223 (1990).
12. The two-step method used for immunoconjugation involves attachment of the heterobifunctional photoreactive cross-linking agent Sulfo-SANPAH to free amino groups on mAb B43 to form a succinimidyl linkage, then photolytic generation of a reactive singlet nitrene on the other terminus of the cross-linker in the presence of a 25-fold molar excess of Gen. The characteristic ultraviolet (UV) absorbance of the nitro-aromatic group of SANPAH was used to monitor the modification of mAb B43 by spectral scanning on a Beckman DU-600 spectrophotometer. Modified B43 was mixed with a 25:1 molar ratio of Gen (Calbiochem, La Jolla, CA) [50 mM solution in dimethyl sulfoxide (DMSO)] and then irradiated with gentle mixing for 10 min with UV light at wavelengths 254 to 366 nm with a multiband UV light–emitter (Model UVGL-15 Mineralight; UVP, San Gabriel, CA). Excess Gen in the reaction mixture was removed by passage through a PD-10 column, and 300-kD B43-B43 homoconjugates with or without conjugated Gen as well as higher molecular weight reaction products were removed by size exclusion high-per-

formance liquid chromatography (HPLC). The final preparation was found to contain, in four independent conjugations, on average one (range, 0.9 to 1.3) molecule of Gen per each mAb B43 molecule, as determined by the specific activity of immunoconjugates prepared with ^{125}I-Gen.

13. To determine the stoichiometry of Gen and antibody in B43-Gen immunoconjugates and to verify the removal of free Gen and Gen-labeled B43-B43 homoconjugates by the described purification procedures, we used ^{125}I-labeled Gen. The specific activity of ^{125}I-Gen was 2.6×10^5 cpm/nmol. The purity of ^{125}I-Gen and B43–^{125}I-Gen immunoconjugate was assessed by SDS–polyacrylamide gel electrophoresis and autoradiography with intensifying screens and Kodak XAR-5 film. The characteristic UV absorbance of the nitro-aromatic group of SANPAH, immunoblot analysis, and ^{125}I-labeling all support the general structure of B43-Gen species shown in Fig. 1A.
14. D. E. Myers and F. M. Uckun, unpublished data. For detailed methodology of ligand-binding assays, see F. M. Uckun *et al.*, *Blood* **70**, 1020 (1987); F. M. Uckun, T. G. Gesner, C. W. Song, D. E. Myers, A. Mufson, *ibid.* **73**, 533 (1989); F. M. Uckun, A. S. Fauci, M.-C. Langlie, J. L. Ambrus, *ibid.* **74**, 761 (1989). The cell lines used in ligand-binding assays included NALM-16, a pre-pre-B leukemia ($CD19^+$-$CD10^+C\mu^-CD20^-mIg^-$); RS4;11 pre-pre-B leukemia ($CD19^+CD10^-C\mu^-CD20^-mIg^-$); NALM-6 pre-B leukemia ($CD19^+CD10^+C\mu^+CD20^-mIg^-$); RAMOS early B-Burkitt's lymphoma-leukemia ($CD19^+CD10^-CD20^+mIg^+$); MOLT-3 T-cell leukemia ($CD7^+CD19^-$); and HL-60 promyelocytic leukemia ($CD19^-CD13^+$). All were maintained in liquid tissue culture [F. M. Uckun *et al.*, *J. Immunol.* **134**, 1504 (1985)].
15. F. M. Uckun, K. G. Waddick, D. E. Myers, unpublished data.
16. Cells (200×10^6) were incubated at 37°C for 18 hours in RPMI medium containing 5% (v/v) calf bovine serum and 1.3 nmol of HPLC-purified B43–^{125}I-Gen (specific activity, 1.8×10^5 cpm/nmol). Subsequently, cells were washed twice in PBS containing 2.5% fetal calf serum to remove unbound radiolabeled material, and the pellets were resuspended in 2.5 ml of 10 mM Hepes, 1 mM EDTA, 0.25 M sucrose (pH 7.5) containing the protease inhibitors aprotinin (10 μg/ml) and leupeptin (10 μg/ml). Homogenization was done with a tight-fitting glass homogenizer, and the mixture was centrifuged at 600*g* for 10 min to pellet nuclei and unbroken cells. The supernatant was layered over 20% Percoll solution (Sigma) in 0.25 M sucrose to fractionate organelles by density gradient centrifugation. An in situ gradient was formed by centrifugation at 22,700*g* for 40 min in a JA-17 rotor (Beckman Instruments). One-milliliter fractions were isolated from the top of the gradient, counted in a gamma counter, and saved for subsequent enzymatic analyses (*17*). Balance tubes contained a mixture of density gradient beads (Pharmacia LKB), layered on top of 20% Percoll in 0.25 M sucrose for calibration of the generated gradients according to the manufacturer's suggestions. Free B43–^{125}I-Gen was also layered over Percoll to indicate the sample loading zone and position of soluble proteins.
17. R. B. Dickson *et al.*, *Biochemistry* **22**, 5667 (1983); J. Manske, thesis, University of Minnesota (1986).
18. F. M. Uckun and D. E. Myers, unpublished data.
19. F. M. Uckun *et al.*, *Proc. Natl. Acad. Sci. U.S.A.* **89**, 9005 (1992).
20. F. M. Uckun and L. T. Ahlgren, unpublished data. Tyrosine phosphorylation was examined by immunoblot analysis as described [F. M. Uckun *et al.*, *Proc. Natl. Acad. Sci. U.S.A.* **88**, 3589 (1991); F. M. Uckun *et al.*, *J. Biol. Chem.* **266**, 17478 (1991)].
21. F. M. Uckun and T. Tedder, unpublished data. cDNAs encoding human CD19 deletion mutants were generated by PCR amplification of the pB4-19 cDNA [T. F. Tedder and C. M. Isaacs, *J. Immunol.* **143**, 712 (1989)] with a series of 3′ antisense oligonucleotides that introduced a stop codon in the coding sequence followed by an Xho I restriction site, and stable K562 transfectants were established as described [L. E. Bradbury, V. S. Goldmacher, T. F. Tedder, *J. Immunol.* **151**, 2915 (1993)].
22. D. E. Myers, L. T. Ahlgren, F. M. Uckun, unpublished data. Kinase renaturation assays were done as described [F. M. Uckun *et al.*, *Proc. Natl. Acad. Sci. U.S.A.* **90**, 252 (1993)].
23. S. H. Kaufmann, *Can. Res.* **49**, 5870 (1989); M. A. Barry, C. A. Behnke, A. Eastman, *Biochem. Pharmacol.* **40**, 2353 (1990); D. Hockenbery *et al.*, *Nature* **348**, 334 (1990); R. A. Lockshin and Z. Zakeri, in *Apoptosis: The Molecular Basis of Cell Death* (Cold Spring Harbor Laboratory Press, Cold Spring Harbor, NY, 1991), pp. 47–60; J. J. Cohen, *Immunol. Today* **14**, 126 (1993).
24. D. I. Cohen *et al.*, *Science* **256**, 542 (1992); C. A. Evans *et al.*, *Can. Res.* **53**, 1735 (1993); H. Otani, M. Erdos, W. J. Leonard, *J. Biol. Chem.* **268**, 22733 (1993).
25. F. M. Uckun and C. W. Song. *Blood* **81**, 1323 (1993).
26. F. M. Uckun *et al.*, *ibid.* **79**, 2201 (1992); F. M. Uckun *et al.*, *ibid.*, p. 3116.
27. D. Z. D'ArGenio and A. Schumitzky, *Comput. Programs Biomed.* **9**, 115 (1979).
28. L. E. Gerlowski and R. K. Jain, *J. Pharmacol. Sci.* **72**, 1103 (1983).
29. F. M. Uckun and L. M. Chelstrom, unpublished data.
30. G. Schieven *et al.*, *Blood* **82**, 1212 (1993); F. M. Uckun, J. Bolen, H. Chae, in preparation.
31. J. Jin and F. M. Uckun, unpublished data.
32. F. M. Uckun and J. A. Ledbetter, *Proc. Natl. Acad. Sci. U.S.A.* **85**, 8603 (1988).
33. F. M. Uckun *et al.*, *Blood* **79**, 3369 (1992).
34. F. M. Uckun, *Br. J. Hematol.* **85**, 435 (1993); ——— and G. Reaman, *Leukemia and Lymphoma*, in press.
35. P. A. Trail *et al.*, *Science* **261**, 212 (1993).
36. I. Pastan *et al.*, *Cell* **47**, 641 (1986); E. S. Vitetta *et al.*, *Science* **238**, 1098 (1988).
37. C. Renner *et al.*, *Science* **264**, 833 (1994).
38. Supported in part by U.S. Public Health Service Grants CA-42633, CA-51425, CA-42111, CA-21737, CA-61549, CA-60437, CA-21765, and CA-13539 from the National Cancer Institute, DHHS; by a Center of Excellence grant from the State of Tennessee; and by American Lebanese Syrian Associated Charities (ALSAC). F.M.U. is a Stohlman Scholar of the Leukemia Society of America. We acknowledge the contributions of Y. Yanishevski to the pharmacodynamic modeling studies.

10 August 1994; accepted 1 December 1994

Suppression of ICE and Apoptosis in Mammary Epithelial Cells by Extracellular Matrix

Nancy Boudreau,* Carolyn J. Sympson, Zena Werb, Mina J. Bissell

Apoptosis (programmed cell death) plays a major role in development and tissue regeneration. Basement membrane extracellular matrix (ECM), but not fibronectin or collagen, was shown to suppress apoptosis of mammary epithelial cells in tissue culture and in vivo. Apoptosis was induced by antibodies to β_1 integrins or by overexpression of stromelysin-1, which degrades ECM. Expression of interleukin-1β converting enzyme (ICE) correlated with the loss of ECM, and inhibitors of ICE activity prevented apoptosis. These results suggest that ECM regulates apoptosis in mammary epithelial cells through an integrin-dependent negative regulation of ICE expression.

Growth, differentiation, and apoptosis are alternative cellular pathways that are each crucial to normal development and the establishment of tissue-specific function. Like growth and differentiation, apoptosis requires active and coordinated regulation of specific genes. In mammalian cells, these genes include *BCL-2*, a homolog of the *Caenorhabditis elegans ced-9* gene, which is a potent suppressor of death (*1*), and *ICE*, a homolog of the *ced-3* gene, which can actively kill cells (*2*). The products of the *BCL-2* and *ICE* genes also appear to function like their *C. elegans* counterparts (*1–3*).

The nature of the ECM can influence the apoptotic program in mammalian cells. Establishment of mammary gland alveolar morphology and expression of milk-specific genes are absolutely dependent on deposition of a laminin-rich ECM (*4*). In addition, involution of the gland, which follows expression of the lactational phenotype, is characterized by degradation of this ECM by metalloproteinases (*5*) and is accompanied by apoptosis (*6*, *7*). Cell attachment, mediated by integrin-ECM interactions, can suppress apoptosis in short-term two-dimensional cultures for up to 30 hours (*8*).

To determine whether ECM regulates apoptosis, we compared the response of CID-9 mammary epithelial cells (MECs) plated directly on tissue culture plastic, in the absence of serum, with those plated on an exogenous basement membrane ECM. Unlike plastic, fibronectin, or type I collagen, this Englebreth-Holm-Swarm (EHS) matrix directs the cells to differentiate, as manifested by the formation of three-dimensional alveolar structures and expression of milk proteins (*9*). After 4 to 5 days on plastic, despite strong adhesion and spreading, the cells began to display char-

N. Boudreau and M. J. Bissell, Life Sciences Division, Lawrence Berkeley Laboratory, 1 Cyclotron Road, Building 83, Berkeley, CA 94720, USA.
C. J. Sympson, Life Sciences Division, Lawrence Berkeley Laboratory, 1 Cyclotron Road, Building 83, Berkeley, CA 94720, USA, and Laboratory of Radiobiology and Environmental Health, University of California, San Francisco, CA 94143, USA.
Z. Werb, Laboratory of Radiobiology and Environmental Health, University of California, San Francisco, CA 94143, USA.
*To whom correspondence should be addressed.